

1 **Shallow water table effects on water, sediment and pesticide** 2 **transport in vegetative filter strips: Part B. model coupling,** 3 **application, factor importance and uncertainty**

4 Claire Lauvernet¹ and Rafael Muñoz-Carpena²

5 ¹Irstea, UR MALY, centre de Lyon-Villeurbanne, 5 rue de la Doua-CS 70077, F-69626 Villeurbanne cedex, France.

6 ²University of Florida, Agricultural and Biological Engineering, 287 Frazier Rogers Hall, PO Box 110570 Gainesville, FL
7 32611-0570, USA

8 *Correspondence to:* Claire Lauvernet (claire.lauvernet@irstea.fr)

9 **Abstract.** Vegetative filter strips are often used for protecting surface waters from pollution transferred by surface runoff in
10 agricultural watersheds. In Europe, they are often prescribed along the stream banks, where a seasonal shallow water table
11 (WT) could decrease the buffer zone efficiency. In spite of this potentially important effect, there are no systematic
12 experimental or theoretical studies on the effect of this soil boundary condition on the VFS efficiency. In the companion
13 paper (Muñoz-Carpena et al., 2017), we developed a physically-based numerical algorithm (SWINGO) that allows
14 representing soil infiltration with a shallow water table. Here we present the dynamic coupling of SWINGO with VFSSMOD,
15 an overland flow and transport mathematical model to study the WT influence on VFS efficiency in terms of reductions of
16 overland flow, sediment and pesticide transport. This new version of VFSSMOD was applied to two contrasted benchmark
17 field studies in France (sandy-loam soil under Mediterranean semi-continental climate, and silty-clay under temperate
18 Oceanic climate), where limited testing of the model with field data on one of the sites showed promising results. The
19 application showed that for the conditions of the studies, VFS efficiency decreases markedly when the water table is 0 to 1.5
20 m from the surface. In order to evaluate the relative importance of WT among other input factors controlling VFS efficiency,
21 global sensitivity and uncertainty analysis (GSA) was applied on the benchmark studies. The most important factors found
22 for VFS overland flow reduction were saturated hydraulic conductivity and WT depth, added to sediment characteristics and
23 VFS dimensions for sediment and pesticide reductions. The relative importance of WT varied as a function of soil type (most
24 important at the silty-clay soil) and hydraulic loading (rainfall + incoming runoff) at each site. The presence of WT
25 introduced more complex responses dominated by strong interactions in the modelled system response, reducing the typical
26 predominance of saturated hydraulic conductivity on infiltration under deep water table conditions. This study demonstrates
27 that when present, WT should be considered as a key hydrologic factor in buffer design and evaluation as a water quality
28 mitigation practice.

29 **1 Introduction**

30 Today, surface waters are threatened by pesticide pollution at the local, regional and global scales (Malaj et al., 2014; Stehle
31 and Schulz, 2015). Agricultural surface runoff is an important contributor to this contamination (Louchart et al., 2001). Grass
32 buffer zones or vegetative filter strips (VFS), are a typical environmental control practice to protect aquatic ecosystems from
33 sediment, and agrichemicals from agricultural fields (Roberts et al., 2012). While VFS are recommended in the USA and
34 other regions, in Europe they are often mandatory along rivers due to their potential to limit surface pesticide runoff and
35 aerial spray drift from entering adjacent surface water bodies (Asmussen et al., 1977; Rohde et al 1980; USDA-NRCS, 2000;
36 Dosskey, 2001; Syversen and Bechmann, 2004; Poletika et al., 2009). However, the effectiveness of edge-of-field buffer
37 strips to reduce runoff transport of pesticides can be very different as a function of many local characteristics (land use, soil,
38 climate, vegetation and pollutant). For example, based on 16 field studies (Reichenberger et al., 2007), the 25th percentile of
39 VFS pesticide reduction efficiency ranges from 45 to 75 % of the amount coming into the filter from the field edge.

40 Moreover, VFS are typically located down the hillslope along the hydrographic network. As a result, the filter is often
41 bounded by a seasonal shallow or perched water table, which may significantly inhibit their function and must be taken into
42 account when designing VFS and evaluating their efficiency (Lacas et al., 2005). Dosskey et al. (2001, 2006) identified
43 presence of shallow water table (<1.8 m) as an important factor that should be considered for VFS design and evaluation.
44 Simpkins et al. (2002) also report that the hydrogeologic setting, specifically the direction of groundwater flow and the
45 position of the water table in thin sand aquifers underlying the buffers, is probably the most important factor in determining
46 buffer efficiency. Arora et al. (2010), in a review on VFS pesticide retention from agricultural runoff present that soil
47 saturation from a shallow water table may be a reason for negative runoff volume retention. Other studies also identify the
48 potential effects of location of the buffers where shallow water table is present (Ohliger and Schulz, 2010; Borin et al., 2004)
49 but do not quantify or study its effects (Lacas et al., 2005).

50 The processes occurring in the VFS interact in a complex manner in space and time, thus they must be simulated by dynamic
51 models accounting for hydrologic (Gatel et al., 2016) and sedimentological variability (Fox et al., 2005). The Vegetative
52 Filter Strip Modeling System (VFSSMOD) (Muñoz-Carpena et al., 1993, 1999; Muñoz-Carpena and Parsons, 2004) is a
53 storm-based numerical model coupling overland flow, water infiltration and sediment trapping in a filter considering
54 incoming surface flow and sediment from an upslope field (Fig. 1). VFSSMOD also includes a generalized empirical pesticide
55 trapping equation as a function of soil and sediment sorption, dissolved phase infiltration, and sorbed phase sedimentation
56 (Sabbagh et al., 2009). Pesticide degradation on the filter is included between runoff events for long-term pesticide
57 assessments (Muñoz-Carpena et al., 2015), but neglected during events due to their short duration (min to h). VFSSMOD has
58 been successfully tested against measured data for predictions of flow, infiltration, and sediment trapping efficiency (Muñoz-
59 Carpena et al., 1999, Abu-Zreig, 2001, Dosskey et al., 2002, Fox et al., 2005, Han et al., 2005, Pan et al., 2017), tracers and

60 multi-reactive reactive solutes (Perez-Ovilla, 2010), phosphorus (Kuo and Muñoz-Carpena, 2009), pesticides (Poletika et al.,
61 2009; Sabbagh et al, 2009; Winchell et al., 2011), and colloids (Yu et al., 2013). Previous work studied the global sensitivity
62 of simulated outflow, sediment and pesticide trapping to VFSMOD input factors (Muñoz-Carpena et al., 2007, 2010, 2015;
63 Fox et al. 2010). At the watershed scale, VFSMOD has been included in methods or frameworks to optimize filter placement
64 and design (Dosskey et al., 2006; Tomer et al., 2009; White and Arnold, 2009; Balderacchi et. al, 2016; Carluer et al., 2017).
65 Sabbagh et al. (2010) integrated VFSMOD within higher-tier, US-EPA long-term pesticide exposure framework
66 (PRZM/VFSMOD/EXAMS) to estimate changes in aquatic concentrations when VFS are adopted as a runoff pollution
67 control practice. Recently, the German EPA (UBA) developed the GERDA software package as a pesticide regulatory tool
68 for surface water that includes VFSMOD simulations with a shallow water table where present (Bach et al., 2017).

69 The extended Green-Ampt soil infiltration component (Skaggs and Khaheel, 1982) used in VFSMOD does not account for
70 the presence of a shallow water table. In a companion paper (Muñoz-Carpena et al., 2017), a physically-based algorithm was
71 developed to describe soil infiltration under shallow water table conditions (SWINGO: Shallow Water table Infiltration
72 alGORithm). Dynamic coupling of this new infiltration algorithm to VFSMOD will allow for mechanistic description of
73 interactions between surface and subsurface hydrology under shallow water table boundary conditions and ensuing effects
74 on VFS sediment and pesticide transport.

75 Thus, the objective of this work is to study the effects that the change in infiltration introduced by the presence of shallow
76 water table has on VFS runoff reduction, sediment and pesticide trapping. This was done by a) dynamic coupling of
77 SWINGO in VFSMOD; b) applying the coupled model on two contrasted and realistic benchmark study sites (sandy-loam
78 soil vs silty-clay soil) and events (Mediterranean semi-continental vs temperate oceanic climates); and c) global sensitivity
79 and uncertainty analysis to ascertain the actual global importance of shallow water table depth on the efficiency of the VFS
80 when compared to other input factors.

81 **2 Material and methods**

82 **2.1 Dynamic coupling of shallow water table infiltration algorithm (SWINGO) with VFSMOD overland flow, 83 sediment and pesticide components**

84 The overland flow submodel in VFSMOD (Muñoz-Carpena et al., 1993a) (Fig. 1) is based on the kinematic wave equation
85 numerical, upwinding Petrov-Galerkin finite element (FE) solution (Lighthill and Whitham, 1955),

$$86 \begin{cases} \frac{\partial h_s}{\partial t} + \frac{\partial q}{\partial x} = i - f = i_e \\ S_f \approx S_o \rightarrow q = \frac{\sqrt{S_o}}{n} h_s^{\frac{5}{3}} \end{cases} \quad (1)$$

87 with initial and boundary conditions

$$88 \quad \begin{cases} h_s = 0; 0 \leq x \leq VL, t = 0 \\ h_s = h_{so}; x = 0, t \geq 0 \end{cases} \quad (2)$$

89 where $h_s = h_s(x, t)$ [L] is the overland flow depth, t is time (L), $q = q(x, t)$ [L^2T^{-1}] is discharge per unit width, x [L] is the surface
90 flow direction axis, $i = i(t)$ [LT^{-1}] is rainfall intensity, $f = f(t)$ [LT^{-1}] is soil infiltration rate, $i_e = i_e(t)$ [LT^{-1}] is rainfall excess, S_o
91 and S_f [LL^{-1}] are the bed and water surface friction slopes at each node of the system, n is Manning's surface roughness
92 coefficient, VL [L] is the filter length, and $h_{so} = h_{so}(0, t)$ [L] represents the field runoff hydrograph entering the filter as a
93 boundary condition (Fig. 2).

94 Originally, the overland flow component was coupled for each time step with a modified Green-Ampt infiltration algorithm
95 for unsteady rainfall (GAMPT, see Fig. 1) for soils without (or with deep) water table (Chu, 1978; Mein and Larson, 1971,
96 1973; Skaggs and Khaheel, 1982; Muñoz-Carpena et al., 1993b). The infiltration component provides the rainfall excess, i_e
97 in Eq. (1), based on a given unsteady rainfall distribution (hyetograph) for each FE node and time step. The field conditions
98 can be well represented since the program handles field inflow hydrographs and hyetographs, and spatial variability of the
99 filter over the nodes of the grid (Fig. 2).

00 In the sediment component (Fig. 1), based on sediment mechanics (transport and deposition) in shallow flow, the model
01 divides the incoming sediment into bed load (coarse particles, with diameter $>37 \mu m$) and suspended load (fine particles,
02 diameter $<37 \mu m$). Bed load deposition is dynamically calculated based on Einstein bed-load transport equation successfully
03 tested for variable shallow flow through non-submerged dense vegetation (Barfield et al., 1978). Transport and deposition of
04 suspended particles is calculated for non-submerged dense vegetation conditions (Tollner et al., 1976; Wilson et al., 1981).
05 Flow characteristics needed for sediment calculations are provided for each time step by the overland flow component. The
06 particle deposition pattern on the filter is predicted based on a conceptual sediment wedge, mass-balance approach (Fig. 2a).

07 Pesticide reduction and transport in the filter during the runoff event is calculated within the water quality/pollutant module
08 (Fig. 1) based on a generalized regression-based approach developed from on a large database of field studies by Sabbagh et
09 al. (2009) and further tested by others (Poletika et al., 2009; Winchell et al., 2011). The equation considers reduction of
10 dissolved pesticide through infiltration, deposition of sediment-bound pesticide, and pesticide adsorption characteristics. The
11 integration of the mechanistic (flow and sedimentation from VFSMOD) and empirical pesticide approaches allows for
12 identification of important site-specific factors determining the efficiency of pesticide removal (or lack of thereof) under
13 realistic field conditions (Muñoz-Carpena et al., 2010; Fox et al., 2010).

14 In this work, to simulate VFS water, sediment and pesticide dynamics under realistic unsteady rainfall-runoff conditions for

15 shallow water table conditions, we dynamically couple the new algorithm SWINGO (developed in the companion paper;
 16 Muñoz-Carpena et al., 2017) as an alternative, user-selected infiltration submodel (Fig. 1). Full details of SWINGO are
 17 provided in the companion paper (Muñoz-Carpena et al., 2017). Briefly, SWINGO is a time-explicit infiltration solution
 18 based on a combination of approaches by Salvucci and Entekhabi (1995) and Chu (1997) with the assumption of a horizontal
 19 wetting front. Proposed integral formulae allow estimation of the singular times: time of ponding (t_p), shift time (t_o), and time
 20 (t_w) when the wetting front depth is equal to z_w (capillary fringe above the water table, Fig. 2b). As with GAMPT, the
 21 algorithm provides the infiltration rate f (Eq. 1) for each FE node and time step in VFSMOD as,

$$22 \quad \begin{cases} f = i & 0 < t < t_p \\ f = f_p = K_s + \frac{1}{z_F} \int_0^{L-z_F} K(h) dh & t_p < t < t_w \\ f = \min(f_w, i) & t \geq t_w \end{cases} \quad (3)$$

23 where (Fig. 2b), z [L] is the vertical axis, z_F [L] is wetting front depth from the surface, L [L] the depth to the water table,
 24 $K=K(h)$ [MT^{-1}] the soil water hydraulic conductivity function of soil matric suction h [L] (non uniform with depth), K_s [MT^{-1}]
 25 is the saturation soil water content, and f_w [MT^{-1}] is the end vertical boundary condition when the wetting front reaches the
 26 water table (or its capillary fringe) typically assumed as vertical saturated flow or lateral drainage (see companion paper for
 27 details; Muñoz-Carpena et al., 2017). For real VFS field situations, unsteady rainfall without initial ponding must be
 28 considered and t_p and t_o calculated. For each time step increment, $\Delta t=t_j-t_{j-1}$, the surface water balance at each VFS FE node
 29 (neglecting evaporation during the event) (Chu, 1997) is,

$$30 \quad \Delta P = \Delta F + \Delta s + \Delta RO \quad (4)$$

31 where ΔP , ΔF , Δs , and ΔRO [L] are changes for each Δt of cumulative precipitation (P), cumulative infiltration (F), surface
 32 storage and cumulative runoff (RO). Notice that $i_e = \Delta RO/\Delta t$ for each time step. Unsteady rainfall is described by a
 33 hyetograph of constant i_j for each rainfall period. If surface storage becomes $s=0$ then t_p and t_o are re-calculated at the next
 34 rainfall period as,

$$35 \quad t_p = \frac{1}{i} (\theta_s z_p - \int_0^{z_p} \theta(L-z) dz) \quad (5)$$

$$36 \quad t_o = \int_0^{z_p} \frac{1}{f_p} [\theta_s - \theta(L-z)] dz \quad (6)$$

37 where θ_s , $\theta(h)$ [L^3L^{-3}] are the soil water saturated content and the soil water characteristic curve, and z_p [L] is the equivalent
 38 wetting front depth at t_p , and for periods after the first, $z_f(t)$ (Fig. 2b) is calculated explicitly from the Newton-Raphson
 39 iterative solution (k iteration level),

$$\begin{aligned}
40 \quad & G(z_F) = t - t_p + t_0 - \int_0^{z_F} \frac{\theta_s - \theta(L-z)}{K_s - \frac{1}{z_F} \int_L^{z_F} K(L-z) dz} dz \Bigg| z_F^{k+1} = z_F^k - \frac{G(z_F^k)}{G'(z_F^k)} \quad \text{with} \quad |z_F^{k+1} - z_F^k| < \varepsilon \quad (7) \\
& G'(z_F) = - \frac{\theta_s - \theta(L-z)}{K_s - \frac{1}{z_F} \int_L^{z_F} K(L-z) dz}
\end{aligned}$$

41 Finally, the algorithm computes t_w , the time to reach column saturation as,

$$42 \quad t_w = t_p - t_0 + \int_0^{z_w} \frac{1}{f_p} [\theta_s - \theta(L-z)] dz \quad (8)$$

43 Similarly, this singular time t_w has to be obtained again each time t_p and t_0 are computed. When initial ponding is present we
44 get $t_p = t_0 = 0$. Additional details are provided in the companion paper (Muñoz-Carpena et al., 2017), and Supp. Materials **S1**
45 provides instructions for downloading the free VFSMOD open source code, documentation and sample applications.

46 **2.2 Benchmark field studies**

47 VFSMOD extended for shallow water table was applied to two experimental VFS sites in France (Fig. 3, Table 1), selected
48 because they represent contrasting agronomic, pedological and climatic conditions (Fontaine 2010). The first site in a
49 Beaujolais vineyard (Rhône-Alpes) consists of a vegetative filter strip on a steep hillslope (20-30%) located along the river
50 Morcille (affluent of the Saône river). The site was instrumented from 2001 to 2008 for long-term experiments of
51 infiltration-percolation of crop protection products (Boivin et al., 2007; Lacas, 2005; Lacas et al., 2012). The region has a
52 semi-continental climate, with Mediterranean influence, where intense seasonal runoff events can induce erosion. The soil is
53 a very permeable granitic sandy-clay. The water table is deep in summer and shallow in winter after intense storm events,
54 from 0.60 m deep at the downstream part of the strip near the river to 4.0 m deep at the field upstream side of the strip
55 (Lacas, 2005).

56 The site of Jaillière (Loire-Atlantique, close to Brittany) is an experimental farm maintained by ARVALIS–Institut du
57 Végétal where soils are shallow and hydromorphic, and climate is temperate oceanic with mild and rainy winters and cool
58 and wet summers (Madrigal-Monarez, 2004). Buffer zone experiments were conducted at the site under natural rainfall
59 (Patty et al., 1997) and simulated runoff (Souiller et al., 2002). Crops are mainly wheat and maize, typically under tile
60 drainage conditions, with slopes of around 3%. Silty clay soils overlay a virtually impermeable layer of alterite shales,
61 typically leading in winter to the formation of seasonal shallow water table from 0.5 m to 2 m and the appearance of runoff
62 by subsaturation (Adamiade, 2004). This site is also the basis for the EU pesticide regulatory scenario for surface water
63 FOCUS_{sw} D5 (EU-FOCUS, 2001).

64 Among the pesticides used at the experimental sites, a soluble and low sorption (mobile) herbicide (isoproturon) used on
65 both sites was selected for simulations, contrasted by a less mobile product chosen at each site, i.e. the fungicide

66 tebuconazole at Morcille and the herbicide diflufenican at Jaillièrre (Madrigal et al 2002) (Table 1).

67 While both Morcille and Jaillièrre provide sufficient details for application of the coupled model (field parameters, initial and
68 boundary conditions), VFS outflow was only available for Morcille. In particular, Lacas (2005) and Lacas et al. (2012)
69 monitored the effectiveness of the VFS at Morcille, but because of the high permeability of the soil and deeper shallow water
70 conditions, only 5 out of the 24 natural rainfall events recorded generated outflow from the VFS. From these 5, the one
71 closer to the average for the high water table season was selected for application of the model (Fig. 4a). Earlier studies at
72 Jaillièrre by Patty et al. (1997) monitored VFS efficiency in the same site but in the absence of a shallow water table.
73 Although they provide some of the model inputs they are not directly applicable for this WT model application. Later,
74 working on the same watershed Branger et al. (2009) and Fontaine (2010) studied the shallow water table effects on runoff at
75 the edge-of-the-field and a receiving drainage ditch, but did not monitor the efficiency of the VFS. We selected one average
76 event (dynamics and volume) in the middle of the high-water season based on Fontaine (2010) for our model application
77 (Fig. 4b).

78 To our knowledge there are no VFS experimental studies with a shallow water table present that can be used for systematic
79 model testing. While this paper focuses on coupling of the new infiltration algorithm with VFSMOD and the analysis of the
80 important factors controlling VFS efficiency in the presence of WT, we used the single event with sufficient hydrological
81 data at Morcille to get a preliminary assessment if the model responds in the same range as the measured field data.
82 Uncalibrated or “cold” testing of the model (without initial calibration using field values) was performed and the 95%
83 confidence interval (grey area in Fig. 4a) was obtained by varying only K_s within measured field values (Table 2). The model
84 performance was assessed against the measured data based on FitEval software (Ritter and Muñoz-Carpena, 2013). FitEval
85 uses block-bootstrapping of the observed and predicted paired values to approximate the underlying distributions of
86 goodness-of-fit statistics (Nash and Sutcliffe Efficiency- NSE and Root Mean Square Error -RMSE). From these
87 distributions, median values and 95% confidence intervals (95CI) are provided for both NSE and RMSE. NSE provides a
88 dimensionless metric of goodness-of-fit, and RMSE an indicator of absolute error, with the same dimensions as model
89 outputs. The uncertainty in the observed data is accounted for in FitEval using the modification of the NSE based on the
90 probable error range (PER) method (Harmel et al, 2007).

91 **2.3 Global sensitivity analysis**

92 Global sensitivity (GSA) and uncertainty analysis (UA) of the coupled model allows for the systematic study of the influence
93 of the input factors and their interactions on VFS performance for surface runoff, sediment and pesticide removal. The
94 “global” term denotes that GSA studies output variability when all input factors vary globally, within their validity domain
95 defined by probability distribution functions (PDF), as opposed to locally, (one at a time), *i.e.* around an arbitrary range from

96 a base value. GSA allows for simultaneous estimation of the factors individual importance and interactions (Saltelli et al.,
97 2004). In this study, two complementary sensitivity methods were used: the qualitative Morris' (1991) elementary effects
98 screening method, and the quantitative variance-decomposition extended Fourier Amplitude Sensitivity Test (eFAST)
99 (Cukier et al., 1978; Saltelli et al., 1999). In both methods, input factors are sampled, the model is evaluated on the sample
00 sets, and global sensitivity indices are computed. Morris is generally used as a first, qualitative step to identify a group of
01 important input factors, where in a second step a variance-based method is applied on the selected input factors (Saltelli et
02 al., 2007, 2008).

03 Morris method uses in its original form a regular discretization of the k input factors space defined by their PDFs, requiring a
04 total number of simulations (N) on the order of $N=r(k+1)$ where $r > 8$ is the number of sampling trajectories, typically taken
05 as 10 used here (Campolongo et al., 2007). Each factor influence, called Elementary Effects (EE), is evaluated by
06 comparison of simulations where this factor is changed alternatively among the others. Morris is a robust, low-cost
07 sensitivity analysis that allows identifying quickly the most influent input factors without prior model assumptions (i.e.
08 linearity, additivity) (Campolongo et al., 2007; Faivre et al., 2013; Khare et al., 2015). Sensitivity indices for each factor X_i
09 ($i=1, k$) are computed based on the EE: (i) μ_i^* (mean of absolute values of EE) that measures *direct effects* of each factor on
10 the output of interest, and (ii) σ_i (standard deviation of EE) that provides a measure of *interactions and non-linearities*. The
11 method compares the input factors' indices relatively to the others, making possible to visually classify the inputs on a (μ^* ,
12 σ) Cartesian plane in 4 groups as a function of their relative effect on the model: (1) negligible effect (low μ^* and low σ); (2)
13 important direct effects and small interactions (high μ^* and low σ); (3) important non-linear and/or interactions (high μ^* and
14 high σ); and (4) interacting factors with low sensitivity (low μ^* and high σ).

15 The eFAST method is a quantitative global sensitivity method based on high-dimensional variance decomposition. A
16 pseudo-random multivariate sampling scheme is conducted across the k -dimensional space, informed by the input factors
17 PDFs, requiring $N=M*k$ simulations with M between 512 and 1024 (8 or 9 binary factor combinations) (Saltelli et. al, 2004).
18 The model total output Y variance is decomposed in parts attributed to each factor direct effects or to factor interactions.
19 First order sensitivity indices (S_i) for each factor X_i are defined by the fraction of the output variance associated to the direct
20 effect of that factor and represents the average output variance reduction that can be achieved when the input factor X_i is
21 fixed (Tarantola et al., 2002; Yang, 2011). Total sensitivity indices (S_{Ti}) are calculated as the fraction of variance associated
22 with that factor and its interactions. The largest values of the sensitivity indices correspond to the highest influence of these
23 inputs on the corresponding output variable (Saltelli et al., 2008; Faivre et al., 2013). eFAST was chosen on this study
24 because it is robust and overcomes the initial limitation of the Fourier Amplitude Sensitivity Test (Cukier et al., 1978)
25 applicable only for mostly additive models (i.e. $\sum S_i > 0.6$) (Faivre et al., 2013). The dense variance-based multivariate
26 sampling and ensuing model simulations allow for quantification of the model uncertainty analysis through output

27 probability density functions and statistics (median, quantiles, confidence intervals) (Saltelli et al. 2004, Muñoz-Carpena et al.
28 2007).

29 Morris indices (μ^* , σ) have been found to provide a good approximation to the eFAST indices (S_{Ti} , S_{Ti-S_i}) at a much lower
30 computational cost (Saltelli et al. 2004, Campolongo et al. 2007) making it ideal for large and computationally expensive
31 models. However, for models with strong non-linear outputs or discontinuities in the output space, the low density of Morris
32 sampling can result in inaccurate sensitivity analysis results. In this study, both methods were run with the full set of inputs
33 as a check for the consistency and robustness of the GSA results. For conciseness, Morris results are presented in detail and
34 eFAST results are summarized briefly with additional details in Supplementary Materials.

35 **2.4 Selection of inputs and outputs for GSA simulations**

36 The first step of GSA is to define output variables and input factors. In this study, changes in VFS efficiency were selected
37 as output variables: reduction of water (dQ), sediments (dE) and pesticides (dP). Both model versions, with water table
38 (SWINGO algorithm) and without water table (GAMPT algorithm), were compared on each site. The input factors (Table 2)
39 were selected considering previous GSA performed on VFSMOD (Fox et al., 2010; Muñoz-Carpena et al., 2007, 2010), with
40 new inputs for the water table case (OR, VGALPHA and VGN, L). Input factors distributions (Table 2) are assigned based
41 either on experimental measurements on the case study plots, scientific publications, or expert knowledge.

42 Although the VFS dimensions FWIDTH and VL were measured on the field (Table 1), the effective dimensions are known
43 to be different in practice as the runoff does not follow perfectly uniform sheet flow (Abu-Zreig, 2001). Thus, the measured
44 values were chosen to vary uniformly within -10% and +10% for FWIDTH and VL, respectively (Muñoz-Carpena et al.,
45 2010). The slope (SOA) uniform distribution represents field measured spatial variation across the VFS. PDFs for filter
46 roughness and vegetation factors were assigned based on vegetation type (Table 1) (Haan et al. 1994; Muñoz-Carpena et al.
47 2007).

48 For the infiltration components, log-normal PDFs were assigned to the soil saturated hydraulic conductivity (VKS) from
49 measured values at each site (Madrigal-Monarez, 2004; Souiller et al., 2002; Lacas, 2005) based on effective field values
50 calculated from the harmonic mean of the topsoil horizons (Bouwer, 1969). The Green-Ampt infiltration OI and OS inputs
51 were fitted distributions based on values measured at the sites, and the average suction at the wetting front (SAV) was
52 considered to vary uniformly based on ranges for soil texture at each site (Rawls et al., 1983). Soil water characteristics
53 parameters (VGALPHA, VGN, OR in Table 2) needed for calculation of infiltration under shallow water table (Eq. 3-8)
54 were assigned normal PDF based on the soil texture (Meyer et al., 1997). Hourly water table depths (L) that were
55 automatically monitored on Morcille during the case study event (Lacas, 2005) followed a uniform distribution. On Jaillièrè,

56 the average water depth and variation was measured manually at the site (Adamiade, 2004) and a uniform distribution
57 around these values assigned.

58 Sediment particle characteristics from the upper field (COARSE and DP) were assigned uniform distributions based on
59 USDA textural class (Woolhiser et al., 1990), and truncated to respect the relationship between DP and COARSE (Muñoz-
60 Carpena et al., 1999).

61 For pesticide inputs, field measurements of the percentage of clay (PTC) and organic carbon (PCTOC) of the upper field
62 followed a uniform PDF (Lacas, 2005; Benoit et al., 1998; Madrigal-Monarez, 2004). The triangular distribution for KOC
63 for the pesticides evaluated at each site is based on measurements; in Jaillière for the base value and boundaries (Benoit et
64 al., 1998; Souiller et al., 2002), and in Morcille for the base value (Lacas, 2005) but using boundaries from PPDB database
65 (IUPAC, 2007).

66 In all, for the two sites, two infiltration options (GAMPT without shallow water table with $k=18$, and SWINGO with shallow
67 water table with $k=20$, Table 2) and 2 pesticides at each site, the total number of GSA simulations performed were 75544 for
68 eFAST ($M=497\approx 500$) and 1600 for Morris. The procedure was repeated 3 times to ensure the robustness of the results.

69 **3. Results**

70 **3.1 Model application on benchmark studies**

71 The effect of water table on simulated VFS efficiency using SWINGO was first tested on the two contrasted benchmark
72 study sites Morcille (Fig. 4a) and Jaillière (Fig. 4b). Since a stream at the bottom of the VFS was present on both sites, the
73 lateral Dupuit-Forscheimer option was selected for the end vertical bottom boundary condition f_w (Eq. 3) (see section 2.1 in
74 companion paper; Muñoz-Carpena et al., 2017), hereon referred to as vertical boundary condition. The detailed outflow
75 hydrograph from the VFS measured during the event at Morcille is compared with a direct simulation with base values (no
76 calibration) (Fig. 4a). The dashed line for $L=2.5$ m corresponds to average measured VKS for the top soil horizons (4.58×10^{-5}
77 m/s), and the grey envelope represents outflow variability due to uncertainty of measured hydraulic conductivity (between
78 3.89×10^{-5} m/s from direct measurement on the soil surface horizon 10-30 cm and 5.29×10^{-5} m/s computed by harmonic
79 mean of measurements on 0-10 cm and 10-30 cm horizons). In addition to the measured water table depth at the sites, each
80 event was tested with different water table conditions to study the response to these conditions (Fig. 4a,b). The large
81 differences in VFS surface outflow found between shallow and deeper water table clearly illustrates the hydrological
82 importance of shallow water table presence on VFS at these sites.

83 Direct simulation of the VFS surface outflow at Morcille fits observations well for the end of the second rain period (4000 to

84 6000s) but misses the rest (Fig. 4a). The differences between simulated and observed values could come from measurement
85 or parametrization errors at the site, since runoff was expected early on for an event with such hydraulic loading (rainfall +
86 incoming runoff). The intrinsic spatial variability of K_s represents also a significant source of uncertainty in the simulations
87 (grey area in Fig. 4a). Nash-Sutcliffe efficiency (NSE) and root mean square error (RMSE) ranges for the model uncertainty
88 bounds in Fig. 4a were median NSE = 0.610 and 95CI [0.448 - 0.943], and RMSE= 4.284×10^{-5} [1.179×10^{-5} - 7.472×10^{-5}]
89 m^3/s . Within those uncertainty bounds, the model is classified as ‘unacceptable’ to ‘very good’ based on the FitEval
90 methodology (Ritter and Muñoz-Carpena, 2013). FitEval evaluation files are included in Supp. Materials. In all, considering
91 that the model was run with base values and without calibration, these preliminary results are deemed satisfactory.

92 The effect of water table change (from 0-2 m) on VFS changes in runoff (dQ), sediment (dE) and pesticide (dP) reductions
93 for the two case studies is presented in Fig. 5. In general, dQ and dP are sensitive to the shallow water table depth until a
94 threshold (~1.5 m for the case study sites) beyond which there are no effects and the filter achieves maximum efficiency for
95 the event. The two-step curves for Morcille are due to the two storm periods, where relative contributions to surface flow
96 between the first and second events will vary with the depth of the shallow water table. Sediment retention (dE) does not
97 exhibit similar changes because the relatively low flow conditions experienced likely result in low transport capacity
98 available and high sediment deposition on the VFS. The difference in effects introduced by the chemical characteristics of
99 the pesticide is observed in the curves for diflufenican (high sorption) and isoproturon (low sorption) at Jaillièrè. This local
00 study does not take into account all effects and interactions between input factors, but only the water table depth variation
01 effect. A global sensitivity analysis presented in section 3.2 will address this.

02 The simulation results for Morcille and Jaillièrè confirm that a shallow water table can affect the VFS surface hydrological
03 response by generating saturation surface runoff, depending on the soil characteristics and the hydraulic loading. Conversely,
04 for deep water table, surface hydrology processes are effectively decoupled after a threshold controlled by the soil
05 characteristics and hydraulic loading. Interestingly, simulations with the no shallow-water table option (GAMPT, Fig. 1) for
06 the case study conditions closely matched those for SWINGO for the deeper water tables in Fig. 4, providing additional
07 physical consistency to both components.

08 **3.2 Global sensitivity analysis of water, sediment and pesticide reductions**

09 A combination of shallow water table (“WT”, run with SWINGO) and no shallow water table (“no WT”, run with GAMPT)
10 simulations (Fig. 1) for Jaillièrè and Morcille conditions with two pesticides at each site (Table 1) were selected for GSA
11 Morris and eFAST methods. For simplicity, GSA results are presented only for one pesticide, isoproturon, which is a
12 common herbicide with average sorption properties. A comparison of the different pesticides effects is presented in the
13 uncertainty analysis section later.

14 Morris sensitivity analysis indices (Table S1 in Supp. Materials) are presented in Fig. 6, where important input factors for
15 each output are separated from the origin of the (μ^* , σ) Cartesian planes. Distinct patterns on the important factors
16 controlling the shallow water table effects on the efficiency of the VFS (dQ, dE, dP) are identified by comparing the
17 different soil (fine at Jaillièrè and coarse at Morcille) and hydraulic loading across the study sites. The differences can be
18 interpreted in terms of the interplay between excess rainfall (controlled mainly by the saturated hydraulic conductivity VKS
19 and hydraulic loading) and sub-saturation (controlled by the water table depth L).

20 Finer soils typically exhibit lower permeability but a higher capillarity fringe above a water table (Terzaghi, 1943; Lane and
21 Washburn, 1946; Parlange et al., 1990). For no WT, excess rainfall (controlled by VKS) leads to relatively more water on
22 the surface compared to coarse soils. Morris results (Fig. 6a) show the strong sensitivity of dQ to VKS for this case. With
23 WT the soil readily saturates from the bottom and it is less sensitive to VKS. This is shown by the strong direct effect of L
24 on dQ (Fig. 6d). For dE in finer soils, more runoff present at the surface typically results in higher transport capacity
25 available, and sediment and surface characteristics become a limiting factor for transport and deposition (Muñoz-Carpena et
26 al., 2010). This is shown by the importance of DP and interaction with VKS (Fig. 6b). With WT, the infiltration is limited
27 even further in these fine soils, where excess rainfall no longer controls surface flow and VKS falls in importance while
28 sediment and surface characteristics dominate the response (Fig. 6e). In general, pesticide reduction (dP) is controlled by
29 factors controlling the liquid (dQ) and solid (dE) phase transport (Sabbagh, et al., 2009). For no WT and for this moderately
30 adsorbed chemical, the effect of excess rainfall on dQ (controlled by VKS) also becomes the most important process for dP
31 (Fig. 6c). With WT, the dominance of L in dQ is also present in dP, with some sediment and pesticide characteristics also
32 showing importance (Fig. 6f).

33 In contrast, the coarser soil in Morcille exhibits higher permeability and small capillary fringe and under no WT runoff is
34 typically controlled by excess rainfall (importance of VKS on Fig. 6g). With WT, the soil might sub-saturate depending on
35 position L and this input gains importance interacting with VKS (Fig. 6j). For dE and no WT (Fig. 6h), with more
36 permeability the surface water flow (controlled by VKS) is the main limiting factor controlling sedimentation (Muñoz-
37 Carpena et al., 2010). With WT, again the VKS and L that control surface flow also interact strongly to control
38 sedimentation, and sediment soil water characteristics are of secondary importance (Fig. 6k). Control of infiltration
39 propagates also into dP, and for this moderately sorbed pesticide, dQ factors also control dP (Fig. 6i,l).

40 Interestingly, introduction of WT increases the number of factors and interactions (i.e. more input factors show higher σ
41 values and are separated near or above the dashed 1:1 line). This indicates an increase in complexity of the VFS response
42 when the shallow water table is present. This suggests that simple relationships to simulate water, sediment and pesticide
43 behavior are not able to represent all complex processes that interact in a VFS.

44 Comparison of Morris and eFAST indices (Fig. 6, and Supp. Mat. Table S2 and Fig. S1) for interactions and first order
45 effects, $S_{Ti}-S_i \sim \sigma$ and $S_{Ti} \sim \mu^*$, respectively, shows good consistency among the methods (Saltelli et al, 2004; Campolongo
46 et al, 2007) and further corroborates the results. The importance of VKS for both soils under no WT identified by Morris is
47 quantified by eFAST with more than 90% of the dQ and dP output variance being controlled by first order (direct) effects of
48 this factor (Fig. S1a,g and c,i). Similarly, the importance of DP for dE for the fine soil is apparent where more than 60% of
49 the variance is explained by first order and interaction effects of this factor (Fig. S1b,e). For the case of WT, the effect of L
50 on dQ and dP is predominant, with 60-90% of the output controlled by this factor and its interactions (Fig. S1d,j,l).

51 **Uncertainty Analysis**

52 The model runs from eFAST dense multivariate input sampling allows realizing a quantitative uncertainty analysis of the
53 model outputs water (dQ), sediment (dE), pesticide (dP) reductions for the 2 contrasted pesticides at each site (Fig. 7 and
54 Table S3 in Supp. Materials). As expected, the reduction in infiltration and increase in surface flow introduced by the
55 shallow water table translates into a distinct decrease in dQ values, with median dQ changing from 81% to 7% and 65% to
56 45% in Jaillière (Fig. 7a, b) and Morcille (Fig. 7c,d), respectively (Table S3, Supp. Materials). For dE, for the coarser soil at
57 Morcille the smaller change in dQ with WT does not visibly change the high sediment retention, whereas for the finer soil of
58 Jaillière the changes in flow introduce marked changes in median dE from 99% to 64%. Again, changes in dQ and dE with
59 WT affect the VFS pesticide retention at both sites, with median reductions from dP = 99% to 38% and 97% to 84% in
60 Jaillière and Morcille, respectively. Since the VFS pesticide retention is also directly related to pesticide sorption
61 characteristics (Sabbagh et al., 2009), some differences are expected for different chemicals. Reduction of diflufenican at
62 Jaillière (dP-Dif) (Fig. 7b) and tebuconazole at Morcille (dP-Teb) (Fig. 7d) is higher than reductions of the other two
63 pesticides because of their affinity for sediment (higher KOC values in Table 1) and high sediment retention in the VFS.

64 These results further support the GSA findings that changes in surface and subsurface hydrological responses introduced by
65 the shallow water table, can translate into important reductions on the expected pesticide retention and uncertainty controlled
66 by field conditions (soils, hydraulic loading, pesticide characteristics).

67 **4. Summary and conclusions**

68 In this study, we coupled a new infiltration algorithm under shallow water table conditions (SWINGO, developed in
69 companion paper; Muñoz-Carpena et al., 2017) with a commonly used event based vegetative filter strips model
70 (VFSSMOD). The coupled model takes into account the dynamic interactions among water table, surface runoff, sediment
71 and pesticide filtration in a vegetative filter strip. The model was applied to two different experimental sites with contrasted
72 soils and rainfall conditions. The direct testing of the uncalibrated model under limited experimental conditions showed

73 promising results. Simulations varying the water table depth for two experimental sites provided interesting insights on the
74 effect on VFS efficiencies to reduce overland flow, sediment and pesticides. While the VFS surface flow, sediment and
75 pesticide reduction responses are very sensitive when the water table is close to the surface, the effect is lost after a threshold
76 depth around 1.5 m for the experimental sites condition, consistent with previous field studies (Dosskey et al., 2006, Lacas et
77 al., 2012). For depths larger than the threshold, the model showed physical consistency when compared to a common Green-
78 Ampt solution (with no water table assumptions). More comprehensive global sensitivity and uncertainty analyses (GSA) for
79 the two sites revealed that the effectiveness of the VFS was markedly reduced in the presence of the shallow water table, and
80 in this case the VFS response is more complex, dominated by interactions between surface, subsurface and transport
81 processes. The most important factors controlling the expected variability of water and pesticide reductions are water table
82 depth and saturated hydraulic conductivity of the soil, but their importance also depends on sediment characteristics
83 controlled by the soil type and hydraulic loading of the event. Uncertainty in the pesticide reduction, driven by water or
84 sediment reduction, also depends on the pesticide sorption properties (Koc).

85 This work suffers from several limitations. Firstly, limited field experimental data is available for detailed studies of
86 the response of a VFS under alternative conditions of deep and shallow water table. Further laboratory and field research
87 should address this limitation, where exhaustive experimental datasets must be compiled to reduce the uncertainty in the
88 identification of sensitive input factors controlling the measured and simulated responses studied here. To address this
89 limitation, a comprehensive laboratory testing of the updated model under mesoscale controlled shallow water conditions
90 was just presented by Fox et al. (2017), with successful results. Still, field studies under controlled and uncontrolled
91 conditions are recommended to identify strategies for model parametrization and optimal design of VFS under realistic WT
92 field conditions. Secondly, although two contrasting case studies were selected, the results presented here are limited to these
93 studies, and further analysis will be needed for other local, regional and larger scales.

94 The application of the improved VFSSMOD under contrasting set of conditions, and physical consistency with other
95 models indicate the robustness of the model for use in VFS sizing and evaluation of potential losses of efficiency under
96 shallow water table conditions. Since VFS are commonly placed near streams and these areas can suffer seasonal shallow
97 water conditions, this tool fills an important gap in environmental management and analysis. For example, in Europe VFS
98 are often prescribed along river drainage networks without objective assessment of their efficiency during winter wet periods
99 (Carluer et al., 2017; Bach et al., 2017). In the US, the historical topography-based approach, which links priority for buffers
00 to locations where runoff water converges from uplands and saturates the soil, often results in placement on bottomlands
01 next to streams (Dosskey and Qiu 2011). Alternative targeted placement of buffers based on soil characteristics and
02 conductivity can improve the efficiency of the buffers (Dosskey et al., 2006). However, both placement methods disregard
03 seasonal shallow water table effects that can now be mechanistically assessed with the improved physical model developed

.04 herein. For the case of the regulatory assessment of pesticides, currently long-term exposure frameworks in Europe and the
.05 USA disregard the potential effects that shallow water effects might have in reducing the effectiveness of in-label mitigation
.06 practices like VFS. Results from this study support the critical need to incorporate in these environmental exposure
.07 assessments the effects of a shallow water table when present.

.08 **Author contribution**

.09 CL and RMC participated in the model coupling, coding the GSA application, analysis and interpretation of the results and
.10 writing of the manuscript.

.11 **Acknowledgements**

.12 The authors wish to thank Nadia Carluer for the field testing dataset and selection of the study sites, and review of the paper.
.13 Marilisa Letey helped with the literature review for this manuscript. Axel Ritter helped in the FitEval evaluation of the
.14 experimental data. CL acknowledges TOPPS-PROWADIS for partial project funding. The second author received support
.15 from the UF Research Foundation Professorship, UF Water Institute Fellowship, and USDA NIFA Award No: 2016-67019-
.16 26855. The authors also thank the University of Florida Research Computing (<http://researchcomputing.ufl.edu>) for
.17 providing high performance computational resources and support that have contributed to the research results reported in this
.18 publication.

19 **References**

- 20 Abu-Zreig, M.: Factors Affecting Sediment Trapping in Vegetated Filter Strips: Simulation Study Using VFSSMOD, *Hydrol.*
21 *Proc.*, 15, 1477, doi:10.1002/hyp.220, 2001.
- 22 Adamiade, V: Influence d'un fossé sur les écoulements rapides au sein d'un versant. Université Pierre et Marie Curie,
23 Spécialité Géosciences - Ressources Naturelles, Paris VI., 2004.
- 24 Arora, K., Mickelson, S.K., Helmers, M.J., Baker, J.L.: Review of Pesticide Retention Processes Occurring in Buffer Strips
25 Receiving Agricultural Runoff. *JAWRA Journal of the American Water Resources Association* 46, 618–647,
26 doi:10.1111/j.1752-1688.2010.00438.x, 2010.
- 27 Asmussen, L.E., White, A.W., Hauser, E.W., Sheridan, J.M.: Reduction of 2,4-D Load in Surface Runoff Down a Grassed
28 Waterway. *J. Environ. Qual.*, 6, 159. doi:10.2134/jeq1977.00472425000600020011x, 1977.
- 29 Balderacchi, M., Perego, A., Lazzari, G., Muñoz-Carpena, R., Acutis, M., Laini, A., Giussani, A., Sanna, M., Kane, D.
30 Trevisan, M.. Avoiding social traps in the ecosystem stewardship: The Italian Fontanile lowland spring. *Sci. Total Env.* 539,
31 526-535, doi:10.1016/j.scitotenv.2015.09.029, 2016.
- 32 Barfield, B. J., E. W. Tollner, and J. C. Hayes: The use of grass filters for sediment control in strip mining drainage. Vol. I:
33 Theoretical studies on artificial media. Pub. No. 35-RRR2-78. Lexington, Ky.: University of Kentucky, Institute for Mining
34 and Minerals Research, 1978.
- 35 Benoit, P., Barriuso, E., Vidon, P., Réal, B.: Isoproturon Sorption and Degradation in a Soil from Grassed Buffer Strip. *J.*
36 *Environ. Qual.*, doi:10.2134/jeq1999.00472425002800010014x, 28,121, 1998.
- 37 Boivin, A., Lacas, J.G., Carluier, N., Margoum, C., Gril, J.-J., Gouy, V.: Pesticide leaching potential through the
38 soil of a buffer strip in the river Morcille catchment (Beaujolais). XIII Symposium Pesticide Chemistry -
39 Environmental Fate and Human Health, Piacenza, Italie, 2007.
- 40 Bouwer, H.: Infiltration of water into nonuniform soil. *Journal of Irrigation and Drainage Division* 95:451–462, 1969.
- 41 Branger, F., Tournebize, J., Carluier, N., Kao, C., Braud, I., Vauclin, M., 2009. A simplified modelling approach for pesticide
42 transport in a tile-drained field: The PESTDRAIN model. *Agricultural Water Management* 96, 415–428.
43 doi:10.1016/j.agwat.2008.09.005

44 Bach M., Guerniche D., Thomas K., Trapp M., Kubiak R., Hommen U., Klein M., Reichenberger S., Pires J., Preuß T.
45 (2017). Bewertung des Eintrags von Pflanzenschutzmitteln in Oberflächengewässer – Runoff, Erosion und Drainage.
46 GERDA - GEobased Runoff, erosion and Drainage risk Assessment for Germany. Umweltbundesamt, Dessau-Roßlau,
47 Germany; ISSN 1862-4359; 553p. [https://www.umweltbundesamt.de/publikationen/bewertung-des-eintrags-von-](https://www.umweltbundesamt.de/publikationen/bewertung-des-eintrags-von-pflanzenschutzmitteln-in)
48 [pflanzenschutzmitteln-in](https://www.umweltbundesamt.de/publikationen/bewertung-des-eintrags-von-pflanzenschutzmitteln-in).

49 Carluer, N., Lauvernet, C., Noll, D., Muñoz-Carpena, R.: Defining context-specific scenarios to design vegetated buffer
50 zones that limit pesticide transfer via surface runoff, *Sci. Total Environ.*, 575, 701-712, doi:10.1016/j.scitotenv.2016.09.105,
51 2017.

52 Chu, S.T.: Infiltration during unsteady rain. *Water Resour. Res.*, 14, 3, 461-466, doi:197810.1029/WR014i003p00461, 1978.

53 Cukier, R.I., Levine, H.B., Shuler, K.E.: Nonlinear sensitivity analysis of multiparameter model systems. *J. Comput.*
54 *Physics*, 26, 1, 1978.

55 Dosskey, M.G.: Toward quantifying water pollution abatement in response to installing buffers on crop land. *Environ*
56 *Manage* 28, 577–598, doi: 10.1007/s002670010245, 2001.

57 Dosskey, M.G., Helmers, M.J., Eisenhauer, D.E.: An Approach for Using Soil Surveys to Guide the Placement of Water
58 Quality Buffers. *Journal of Soil and Water Conservation* 61, 344–354, 2006.

59 Dosskey, M.G., M.J. Helmers, D.E. Eisenhauer, T.G. Franti and K.D. Hoagland: Assessment of concentrated flow through
60 riparian buffers. *Journal of Soil and Water Conservation*, 57:336–343, 2002.

61 Dukes, M.D., Evans, R.O., Gilliam, J.W., Kunickis, S.H.: Effect of Riparian Buffer Width and Vegetation Type on Shallow
62 Groundwater Quality in the Middle Coastal Plain of North Carolina, *Trans. of ASABE* 45:327, 2002.

63 EU-FOCUS. 2001. FOCUS Surface Water Scenarios in the EU Evaluation Process under 91/414/EEC. Report of the
64 FOCUS Working Group on Surface Water Scenarios, EC Document Reference SANCO/4802/2001 –rev .2. 245pp, Version
65 1.0, January 2011.

66 EU-JRC. 2004. SIMLAB Version 2.2.1. Simulation Environment for Uncertainty and Sensitivity Analysis. Joint Research
67 Centre of the European Commission, Ispra, Italy. <https://ec.europa.eu/jrc/en/samo/simlab> (accessed July 2017)

68 Faivre, R., Iooss, B., Mahévas, S., Makowski, D., Monod, H.: Sensitivity Analysis and Exploration of Models. Editions
69 Quae, in French, 2013.

.70 Fontaine, A.: Optimizing the size of grassed buffer strips to limit pesticides transfer from land to surface water in overland
.71 flow », Cranfield University, UK, MSc Thesis, 2010.

.72 Fox, A.L., D.E. Eisenhauer, M.G. Dosskey: Modeling water and sediment trapping by vegetated filters using VFSSMOD:
.73 comparing methods for estimating infiltration parameters. ASAE Paper, 052118. Joseph, 2005.

.74 Fox, G., Muñoz-Carpena, R., Sabbagh, G.: Influence of flow concentration on parameter importance and prediction
.75 uncertainty of pesticide trapping by vegetative filter strips. *J. Hydrol.*, 384, 164-173, doi:10.1016/j.jhydrol.2010.01.020,
.76 2010.

.77 Fox, G., R. Muñoz-Carpena and R. Purvis. Controlled laboratory experiments and modeling of vegetative filter strips with
.78 shallow water tables. *J. of Hydrology*, doi:10.1016/j.jhydrol.2017.10.069, 2017.

.79 Gatel, L., Lauvernet, C., Carlier, N., and Paniconi, C.: Effect of surface and subsurface heterogeneity on the hydrological
.80 response of a grassed buffer zone, *Journal of Hydrology*, 542, 637-647, 10.1016/j.jhydrol.2016.09.038, 2016.

.81 Haan CT, Barfield BJ, Hayes JC.: Design hydrology and sedimentology for small catchments. San Diego, Calif.: Academic
.82 Press, 1994.

.83 Han, J., Wu, S., Allan, C.: Suspended sediment removal by vegetative filter strip treating highway runoff. *Journal of*
.84 *Environmental Science and Health*, 40:1637–1649, doi:10.1081/ESE-200060683, 2005.

.85 Harmel, R. D., and P. K. Smith. 2007. Consideration of measurement uncertainty in the evaluation of goodness- of- fit in
.86 hydrologic and water quality modeling. *J. Hydrol.* 337(3- 4): 326- 336.

.87 Johnson, S.R., Burchell, M.R. R.O. Evans, D.L. Osmond, Gilliam, J.W.: Riparian Buffer Located in an Upland Landscape
.88 Position Does Not Enhance Nitrate-Nitrogen Removal, *Ecol. Engineering*, 52, 252, doi:10.1016/j.ecoleng.2012.11.006,
.89 2013.

.90 Khare, Y.P., R. Muñoz-Carpena, R.W. Rooney. and C.J. Martinez: A multi-criteria trajectory-based parameter sampling
.91 strategy for the screening method of elementary effects. *Environ. Modell. Softw.* 64,230-239,
.92 [doi:10.1016/j.envsoft.2014.11.013](https://doi.org/10.1016/j.envsoft.2014.11.013), 2015.

.93 Kuo, Y.M. and R. Muñoz-Carpena: Simplified modeling of phosphorus removal by vegetative filter strips to control runoff
.94 pollution from phosphate mining areas, *J. of Hydrol.*, 378, 343-354, doi:10.1016/j.jhydrol.2009.09.039, 2009.

- 95 Lacas, J.-G., 2005. Processus de dissipation des produits phytosanitaires dans les zones tampons enherbées. Etude
96 expérimentale et modélisation en vue de limiter la contamination des eaux de surface. Université Montpellier II. Sciences et
97 techniques du Languedoc.
- 98 Lacas, J.-G., Voltz, M., Gouy, V., Carluer, N., Gril, J.-J.: Using grassed strips to limit pesticide transfer to surface water: a
99 review. *Agron. Sustain. Dev.* 25, 253–266, doi:10.1051/agro:2005001, 2005.
- 00 Lacas, J.-G., Carluer, N., Voltz, M.: Efficiency of a Grass Buffer Strip for Limiting Diuron Losses from an Uphill Vineyard
01 Towards Surface and Subsurface Waters. *Pedosphere*, 22, 580-592, doi:10.1016/S1002-0160(12)60043-5, 2012.
- 02 Lane, K. S., and Washburn, S. E.: Capillary tests by capillarimeter and by soil filled tubes. *Proc. Highway Research Board*,
03 26, 460–473, 1946.
- 04 Lighthill, M.J., Whitham, C.B.: On kinematic waves: flood movement in long rivers. *Proc. R. Soc. London Ser. A* , 22, 281-
05 316, 1955.
- 06 Louchart, X., M. Voltz, P. Andrieux, et R. Moussa: Herbicide Transport to Surface Waters at Field and Watershed Scales in
07 a Mediterranean Vineyard Area, *Journal of Environmental Quality*, 30:982, 2001.
- 08 Madrigal-Monarez, I.: Sorption of pesticides in soil from grassed and forested buffer zones: the role of organic matter.
09 INAPG PhD Thesis (AgroParisTech), 2004.
- 10 Malaj E., P.C. von der Ohe, M. Grote, R. Kühne, C.P. Mondy, P. Usseglio-Polatera, W. Brack, and R.B. Schäfer. Organic
11 chemicals jeopardize the health of freshwater ecosystems on the continental scale. *PNAS* 111, 26, 9549-9554.
12 doi:10.1073/pnas.1321082111, 2014.
- 13 Mein, R.G., Larson, C.L.: Modelling the infiltration component of the rainfall-runoff process, Bulletin 43, University of
14 Minnesota, MN, Water Resources Research Center, 1971.
- 15 Meyer, P.D.; Rockhold, M.L. & Gee, G.W. Uncertainty analyses of infiltration and subsurface flow and transport for SDMP
16 sites, report, September 1, 1997; Washington D.C.. (digital.library.unt.edu/ark:/67531/metadc690558/: accessed July 7,
17 2017), University of North Texas Libraries, Digital Library, digital.library.unt.edu; crediting UNT Libraries Government
18 Documents Department.
- 19 Muñoz-Carpena, R., C.T. Miller, and J.E. Parsons: A Quadratic Petrov-Galerkin Solution for Kinematic Wave Overland
20 Flow. *Water Resour. Res.* 29, 8, 2615-2627, 1993a.

- 21 Muñoz-Carpena, R., Parsons, J.E., Gilliam, J.W.: Numerical Approach to the Overland Flow Process in Vegetative Filter
22 Strips, *Trans. of ASABE* 36, 3, 761-770, 1993b.
- 23 Muñoz-Carpena, R., Parsons, J.E., Gilliam, J.W.: Modeling hydrology and sediment transport in vegetative filter strips. *J.*
24 *Hydrol.*, 214, 111–129. doi:10.1016/S0022-1694(98)00272-8, 1999.
- 25 Muñoz-Carpena, R. and Parsons, J. E.: A design procedure for vegetative filter strips using VFSSMOD-W, *Transactions of*
26 *the ASAE* 47(6), 1933—1941, doi :10.13031/2013.17806, 2004.
- 27 Muñoz-Carpena, R., Z. Zajac, et Y.-M. Kuo: Global sensitivity and uncertainty analyses of the water quality model
28 VFSSMOD., *Trans. of ASABE* 50:1719–1732, 2007.
- 29 Muñoz-Carpena, R., Fox, G., Sabbagh, G.: Parameter Importance and Uncertainty in Predicting Runoff Pesticide Reduction
30 with Filter Strips. *Journal of Environmental Quality*, 39,630, doi:10.2134/jeq2009.0300, 2010.
- 31 Muñoz-Carpena, R. A. Ritter, G.A. Fox and O. Perez-Ovilla: Does mechanistic modeling of filter strip pesticide mass
32 balance and degradation affect environmental exposure assessments? *Chemosphere* 139:410-421.
33 [doi:10.1016/j.chemosphere.2015.07.010](https://doi.org/10.1016/j.chemosphere.2015.07.010), 2015.
- 34 Muñoz-Carpena, R., Lauvernet, C., and Carluer, N. Shallow water table effects on water, sediment and pesticide transport in
35 vegetative filter strips: Part A. non-uniform infiltration and soil water redistribution, *Hydrol. Earth Syst. Sci. Discuss.*,
36 doi:10.5194/hess-2017-405, in review, July 2017.
- 37 Ohliger, R., Schulz, R.: Water body and riparian buffer strip characteristics in a vineyard area to support aquatic pesticide
38 exposure assessment, *Sci. Total Environ.*, 408, 5405-5413, doi:10.1016/j.scitotenv.2010.08.025.
- 39 Pan, D.; Gao, X.; Dyck, M.; Song, Y.; Wu, P., Zhao, X.: Dynamics of runoff and sediment trapping performance of
40 vegetative filter strips: Run-on experiments and modeling *Science of The Total Environment*, 593–594, 54-64,
41 [doi:10.1016/j.scitotenv.2017.03.158](https://doi.org/10.1016/j.scitotenv.2017.03.158), 2017.
- 42 Parlange, J.-Y., Haverkamp, R., Starr, J. L., Fuentes, C., Malik, R. S., Kumar, S., and Malik, R. K.: Maximal capillary rise
43 flux as a function of height from the water table. *Soil Sci.*, 150, 6, 896–898, 1990.
- 44 Patty, L., Réal, B., Gril, J.J.: The use of grassed buffer strips to remove pesticides, nitrate and soluble phosphorus
45 compounds from runoff water. *Pesticide science*, 243:251, 1997.

46 Perez-Ovilla, O.: Modeling runoff pollutant dynamics through vegetative filter strips: a flexible numerical approach. Ph.D.
47 Thesis, University of Florida, Gainesville, 195pp, 2010.

48 Poletika, N.N., Coody, P.N., Fox, G.A., Sabbagh, G.J., Dolder, S.C., White, J.: Chlorpyrifos and Atrazine Removal from
49 Runoff by Vegetated Filter Strips: Experiments and Predictive Modeling. *J. Environ. Qual.*, 38, 1042–1052.
50 doi:10.2134/jeq2008.0404, 2009.

51 Rawls W.J., Brakensiek D.L., Miller N.: Green-Ampt infiltration parameters from soils data. *J. Hydraul. Eng.*, 109(1), 62-70,
52 1983.

53 Reichenberger S., Bach M., Skitschak A., Frede H.-G.: Mitigation strategies to reduce pesticide inputs into ground- and
54 surface water and their effectiveness: a review. *Sci. Total Environ.*, 384, 1-35, doi:10.1016/j.scitotenv.2007.04.046, 2007.

55 Ritter, A. and R. Muñoz-Carpena. 2013. Predictive ability of hydrological models: objective assessment of goodness-of-fit
56 with statistical significance. *J. of Hydrology* 480(1):33-45. doi:10.1016/j.jhydrol.2012.12.004

57 Roberts, W.M., M.I. Stutter, and P.M. Haygarth: Phosphorus Retention and Remobilization in Vegetated Buffer Strips: A
58 Review. *J. Environ. Qual.* 41:389–399 (2012) doi:10.2134/jeq2010.0543, 2012.

59 Rohde, W.A., L.E. Asmussen, E.W. Hauser, R.D. Wauchope: Trifluralin movement in runoff from a small agricultural
60 watershed. *J. Environ. Qual.*, 9, pp. 37–42, 1980.

61 Sabbagh, G.J., Fox, G.A., Kamanzi, A., Roepke, B., Tang, J.-Z.: Effectiveness of Vegetative Filter Strips in Reducing
62 Pesticide Loading: Quantifying Pesticide Trapping Efficiency. *J. Environ. Qual.* 38, 762. doi:10.2134/jeq2008.0266, 2009.

63 Saltelli A., S. Tarantola, F. Campolongo, M. Ratto: *Sensitivity Analysis in Practice: A Guide to Assessing Scientific Models.*
64 John Wiley & Sons, Chichester, 2004.

65 Saltelli, A., Annoni, P., Azzini, I., Campolongo, F., Ratto M., Tarantola, S.: Variance Based Sensitivity Analysis of Model
66 Output. Design and Estimator for the Total Sensitivity Index. *Computer Physics Communications* 181:259, 2010.

67 Saltelli, A., Ratto, M., Andres, T., Campolongo, F., Cariboni, J., Gatelli, D., Saisana, M., Tarantola, S.: *Global Sensitivity*
68 *Analysis: The Primer.* John Wiley & Sons, Chichester, 2008.

69 Saltelli, A., Tarantola, S., Chan, K.P.-S.: A Quantitative Model-Independent Method for Global Sensitivity Analysis of
70 Model Output, *Technometrics* 41:39, 1999.

71 Simpkins, W., Wineland, T., Andress, R., Johnston, D., Caron, G., Isenhardt, T., Schultz, R. : Hydrogeological constraints on
72 riparian buffers for reduction of diffuse pollution: examples from the Bear Creek watershed in Iowa, USA, *Water Science
73 and Tech.* 45, 9, 2002.

74 Skaggs, R.W., Khaheel, R., 1982. Infiltration, Ch. 4, In: *Hydrologic modeling of small watersheds*. C.T. Haan, H.P. Johnson,
75 D.L. Brakensiek, Eds., St. Joseph, MI, ASAE. pp. 121–168.

76 Souiller, C., Y. Coquet, V. Pot, P. Benoit, B. Réal, C. Margoum, B. Laillet, C. Labat, P. Vachier, A. Dutertre: Capacités de
77 stockage et d'épuration des sols de dispositifs enherbés vis-à-vis des produits phytosanitaires. Première partie : Dissipation
78 des produits phytosanitaires à travers un dispositif enherbé ; mise en évidence des processus mis en jeu par simulation de
79 ruissellement et infiltrométrie. *Etude et Gestion des Sols*, 9,269, 2002.

80 Stehle, S., and R. Schulz: Agricultural insecticides threaten surface waters at the global scale. *PNAS* 112, 18, 5750-5755,
81 doi:10.1073/pnas.1500232112, 2015.

82 Syversen, N. and M. Bechmann: Vegetative buffer zones as pesticide filters for simulated surface runoff. *Ecological
83 Engineering* 22:175–184, 2004.

84 Tarantola, S., N. Giglioli, J. Jesinghaus, et A. Saltelli: Can Global Sensitivity Analysis Steer the Implementation of Models
85 for Environmental Assessments and Decision-Making? *Stochastic Environmental Research and Risk Assessment*, 16, 63,
86 2002.

87 Terzaghi, K.: *Theoretical soil mechanics*, Wiley, New York, 1943.

88 Tollner, E.W., Barfield, B.J, Haan, C.T., Kao, T.Y.: Suspended sediment filtration capacity of simulated vegetation. *Trans.
89 ASAE* 19, 4, 678-682, 1976.

90 Tomer, M.D., M.G. Dosskey, M.R. Burkart, D.E. James, M.J. Helmers and D.E. Eisenhauer: Methods to prioritize
91 placement of riparian buffers for improved water quality. *Agroforestry Systems* 75, 1, 17-25, 2009.

92 IUPAC: The PPDB Pesticide Properties Database. International Union of Pure and Applied Chemistry (IUPAC), AERU,
93 University of Hertfordshire, UK. <http://sitem.herts.ac.uk/aeru/ppdb/en/index.htm>), 2007.

94 Winchell, M.F., Jones, R.L., Estes, T.L.: Comparison of models for estimating the removal of pesticides by vegetated filter
95 strips. *ACS Symp. Ser.* 273-286, 2011.

- 96 Woolhiser, D.A., R.E. Smith, et D.C. Goodrich: KINEROS, A kinematic runoff and erosion model: documentation and user
97 manual, 1990.
- 98 Yang, J.: Convergence and uncertainty analyses in Monte-Carlo based sensitivity analysis. *Environ. Modell. Softw.* 26:444,
99 2011.
- 00 Yu, C., R. Muñoz-Carpena, B. Gao and O. Perez-Ovilla: Effects of ionic strength, particle size, flow rate, and vegetation
01 type on colloid transport through a dense vegetation saturated soil system: Experiments and modeling. *J. of Hydrology*, 499,
02 316-323, doi:10.1016/j.jhydrol.2013.07.004, 2013.
- 03 White, M. J. and Arnold, J. G.: Development of a simplistic vegetative filter strip model for sediment and nutrient retention
04 at the field scale, *Hydrol. Proc.*, 23, 11, doi:10.1002/hyp.7291, 2009.

Table 1. Characteristics of the field studies utilized for sensitivity–uncertainty analyses of shallow water table effects on VFS performance

Study	Authors	Lacas (2005); Lacas et al. (2012)	Madrigal-Monarrez (2004), Adamiade (2004)
	Location, climate	Morcille, Mediterranean semi-continental	Jaillère, Temperate oceanic
Event description	Rainfall (mm)	15	10.7
	Rainfall duration (hr)	2.1	3
	Inflow volume (mm)	0.847	6.347
	Inflow duration (hr)	2.1	7.9
	Hydraulic loading (rainfall + incoming runoff) (m ³)	2.48	25.9
	Shallow water table depth (m)	2.5 (0.4-2.5)	0.8 (0.4-2)
	Source field area (m ²)	2500	4000
Soil description	USDA Soil Taxonomy	Cambisol-luvic	Stagnic-luvisol
	USDA texture	Sandy-loam	Silty-clay
VFS description	Length (direction of flow)×width	6 x 4m	5 x 10m
	slope	28%	4%
	Field-to-filter area ratio	110	100
	Vegetation	Ray-grass (20 years)	Ray-grass (7 years)
Pesticides (K _{oc} , ml/g)		isoproturon (144)	isoproturon (144)
		tebuconazole (769)	diflufenican (3000)

608 Table 2. Input factors base values and selected statistical distributions at the case study sites.

Input factor (units)	Description	Morcille		Jaillière	
		Base value	Distribution	Base value	Distribution
Hydrological inputs					
FWIDTH (m)	Effective flow width of the strip	4.0	$U(4.0, 4.4)$	10.0	$U(9.0, 10.0)$
VL (m)	Length in the direction of the flow	6.0	$U(5.4, 6.0)$	5.0	$U(5.0, 5.5)$
RNA ($s\ m^{-1/3}$)	Filter Manning's roughness n for each segment	0.2	$T(0.1, 0.2, 0.3)$	0.2	$T(0.1, 0.2, 0.3)$
SOA (-)	Filter slope for each segment	0.25	$U(0.20, 0.30)$	0.03	$U(0.02, 0.04)$
VKS ($m\ s^{-1}$)	Soil vertical saturated hydraulic conductivity in the VFS	4.58E-5	$LN(-10.6676, 0.69)$	2.50E-6	$LN(13.0, 0.69)$
SAV (m)	Green-Ampt's average suction at wetting front	0.110	$U(0.088, 0.132)$	0.1668	$U(0.13, 0.20)$
OI (-)	Initial soil water content, θ_i	0.22	$U(0.1, 0.35)$	0.15	$U(0.12, 0.18)$
OS (-)	Saturated soil water content, θ_s	0.4	$N(0.4, 0.03)$	0.4	$N(0.4, 0.03)$
SCHK (-)	Relative distance from the upper filter edge where check for ponding conditions is made (i.e., 1 = end; 0 = beginning)	0.5	$U(0, 1)$	0.5	$U(0, 1)$
L (m) [†]	Shallow water table depth from soil surface	1.0	$U(0.4, 2.5)$	0.8	$U(0.4, 2)$
OR (-) [†]	Residual soil water content, θ_i	0.038	$N(0.038, 0.03)$	0.07	$N(0.07, 0.03)$
VGALPHA (m^{-1}) [†]	van Genuchten soil characteristic curve parameter (α)	10.0	$N(10, 2)$	1.18	$N(1.18, 0.05)$
VGN (-) [†]	van Genuchten soil characteristic curve parameter (n), $m=1-1/n$	1.52	$N(1.52, 0.05)$	1.45	$N(1.45, 0.05)$
Vegetation inputs					

SS (cm)	Average spacing of grass stems	1.6	$U(1.3,2.1)$	1.6	$U(1.3,2.1)$
VN ($s\text{ cm}^{-1/3}$)	Filter media (grass) modified Manning's n_m (cylindrical =0.012)	0.012	$T(0.0084,0.012,0.016)$	0.012	$T(0.0084,0.012,0.016)$
H (cm)	Filter grass height	15.0	$U(10,35)$	15.0	$U(10,35)$
Sedimentation inputs					
VN2 ($s\text{ m}^{-1/3}$)	Bare surface Manning's n for sediment inundated area in VFS	0.013	$T(0.011,0.013,0.04)$	0.02	$T(0.011,0.02,0.04)$
DP (cm)	Sediment particle size diameter (d_{50})	0.0099	$U(3.80E-3,1.60E-2)$	0.0029	$U(2.00E-4,3.69E-3)$
COARSE (-)	Fraction of incoming sediment with particle diameter > 0.0037 cm (coarse fraction routed through wedge as bed load) [unit fraction, i.e. 100% = 1.0]	0.55	$U(0.51,0.6)$	0.45	$U(0.4,0.49)$
Pesticide inputs					
KOC (ml/g)	Organic carbon sorption coefficient for simulated pesticide				
Isoproturon		144	$T(36,144,241)$	144	$T(36,144,241)$
Tebuconazole		769	$T(102, 769,1249)$	–	–
Diflufenican		–	–	3000	$T(1622,3000,7431)$
PCTOC (%)	Percentage of organic carbon in the soil	1.2	$U(1.18,2.5)$	3.78	$U(1.4,7)$
PCTC (%)	Percentage clay in the soil	12	$U(11,15)$	22	$U(19.8,25.5)$

609 † Parameters of the new infiltration under shallow water table component (SWINGO); ‡Statistics of the assigned distributions, uniform: $U(\text{min},\text{max})$, triangular:
610 $T(\text{min},\text{mean},\text{max})$, log-normal: $LN(\mu_y,\sigma_y)$, normal: $N(\mu_x,\sigma_x)$. LN and N distributions are truncated between (0.001,0.999).

611 **Figure captions**

612 **Figure 1: Conceptual model of VFSSMOD showing the coupling between overland flow, soil infiltration and**
613 **redistribution, sediment and pesticide components. Solid lines indicate required processes and their interactions, and**
614 **dashed lines are optional, user selected components. The selection of infiltration under either a) deep water table**
615 **(extended Green-Ampt, GAMPT), or b) shallow water table (SWINGO) is highlighted.**

616 **Figure 2: Details of the dynamic coupling of (a) the overland flow and sediment and pesticide transport through the**
617 **VFS (contained in VFSSMOD), with (b) the new infiltration and soil water redistribution with shallow water**
618 **component (SWINGO). Colors indicate water (blue), sediment (brown) and pesticide (red) components. V , M and m**
619 **indicate water, sediment and pesticide mass moving through the filter, where subscripts indicate incoming (i),**
620 **outgoing (o), in sediment (sed), on the filter (f), infiltrated (F), in mixing-layer (ml) and in runoff (ro). Other symbols**
621 **are defined in the text.**

622 **Figure 3: Location of experimental VFS sites: Jailli re, North-West of France, maize crops on a flat silty-clay soil**
623 **under Temperate oceanic climate; Morcille, South-East of France, vineyards on a sandy-loam soil under**
624 **Mediterranean semi-continental climate. Morcille is located at 46 10'31.3"N - 4 38'11.2"E and Jailli re at**
625 **47 27'6.25"N - 0 57'58.37"O, in GPS coordinates.**

626 **Figure 4: Hydrological response of the VFS at the study sites. (a) Event at Morcille Aug. 17, 2004 with $L=2.5$ m,**
627 **showing comparison of measured outflow (symbols) and VFSSMOD simulations (lines). The dashed Q_{out} line for $L=2.5$**
628 **m corresponds to average conditions for that event ($K_s = 4.58E-05$ m/s), and the grey envelope represents outflow**
629 **variability due to uncertainty of measured hydraulic conductivity. (b) Event at Jailli re on February 16, 1997 with**
630 **$L=0.8$ m, without outflow measurements. Q_{in} and Q_{out} represent surface inflow and outflow at the VFS. The**
631 **potential effect on overland outflow of alternative water table depths in those events is represented by the dotted lines**
632 **for $L=0.4$ (a) and 4.0 m (b).**

633 **Figure 5: Change in dQ (reduction of surface water), dE (reduction of sediment) and dP (reduction of pesticide**
634 **isoproturon) with water table depth for experimental events in Fig. 4a-b. Grey area indicates water table depths**
635 **where influence over surface outputs on the VFS is no longer observed.**

636 **Figure 6: Morris elementary effects results for dQ (reduction of surface water), dE (reduction of sediment) and dP**
637 **(reduction of pesticide isoproturon) on Jailli re (a-f) and Morcille (g-l) sites, without water table (no WT) and with**
638 **water table (WT) present. Factors with negligible effects (close to the origin) are not labeled.**

639 **Figure 7: Probability density functions from the uncertainty analysis of eFAST simulations on output variables dQ**
640 **(reduction of surface water), dE (reduction of sediment), dP (reduction of pesticides) for the Jailli re (a-b) and**
641 **Morcille (c-d) sites, without water table (no WT) and with water table (WT). Pesticides are isoproturon (Iso),**
642 **diflufenican (Dif) and tebuconazole (Teb).**

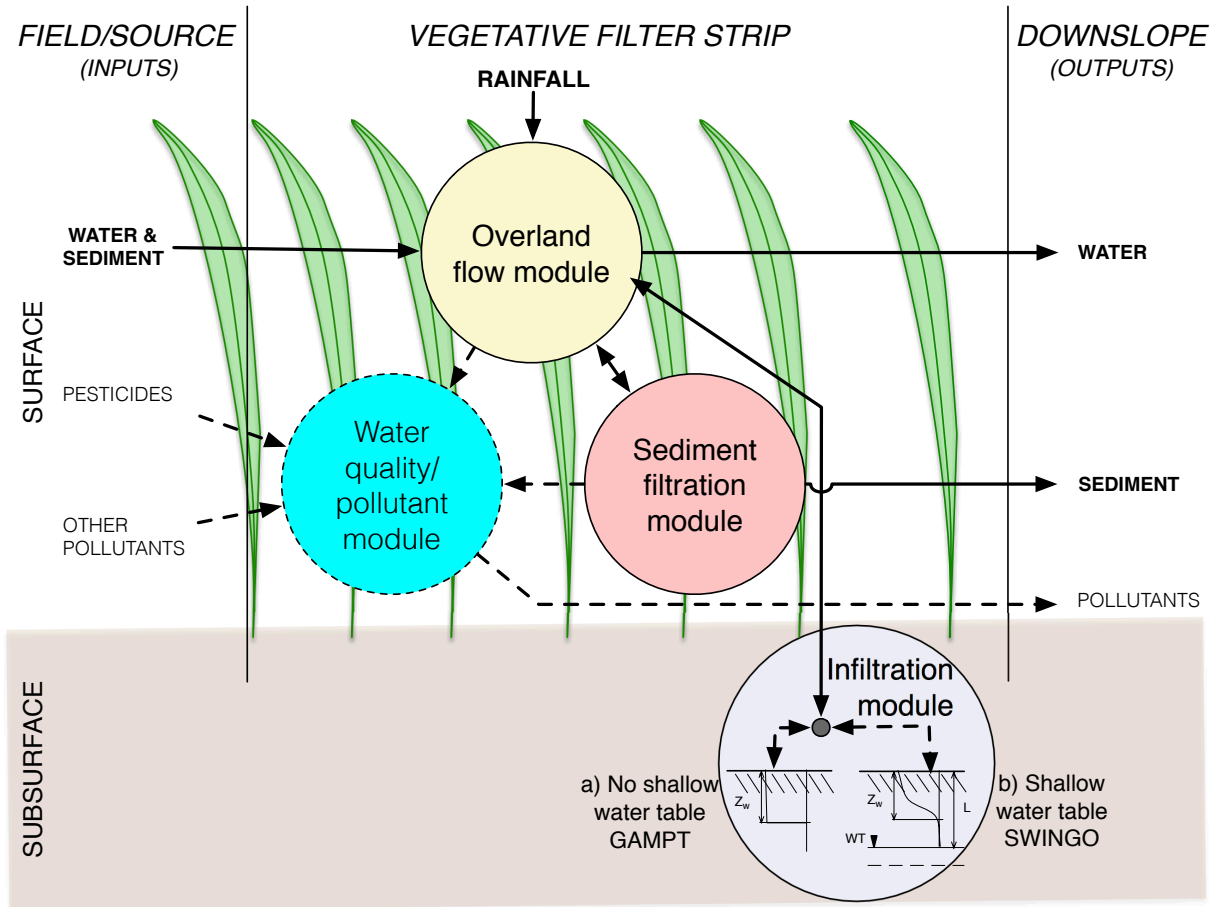


FIG. 1

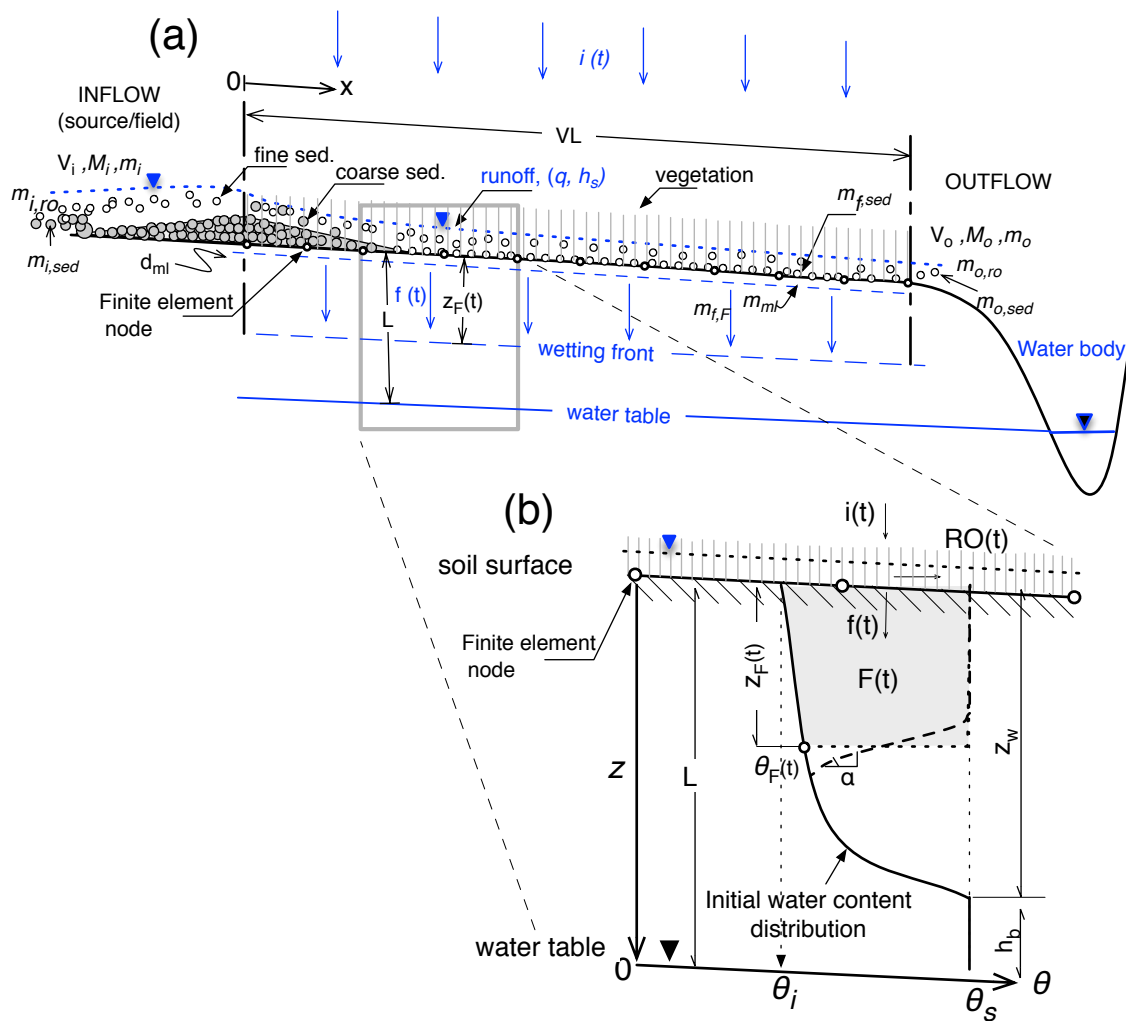


FIG. 2

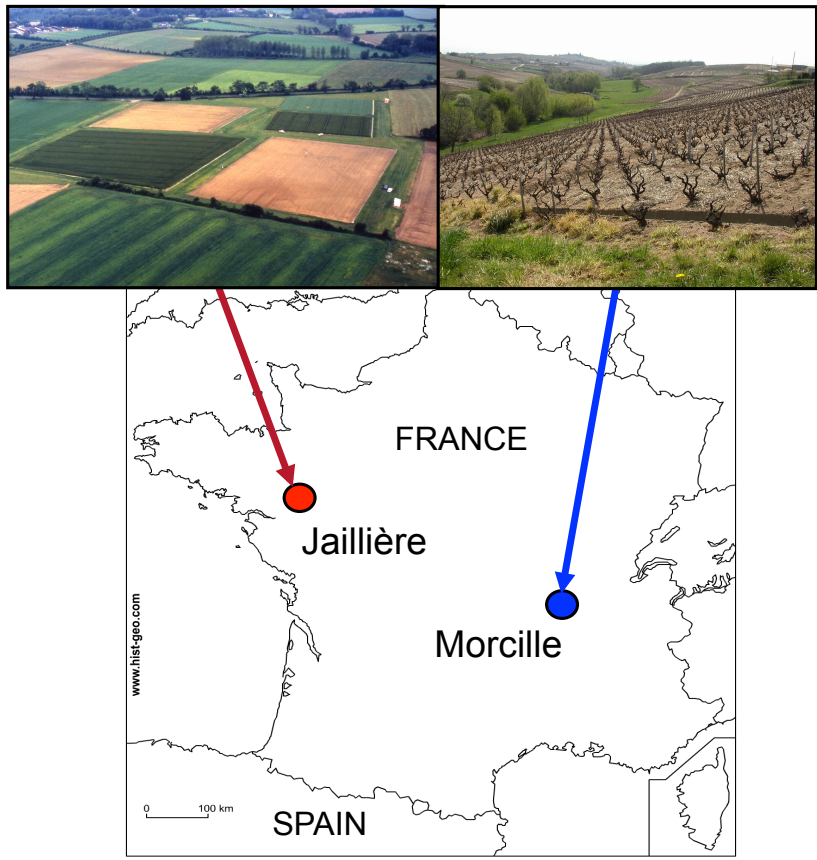


FIG. 3

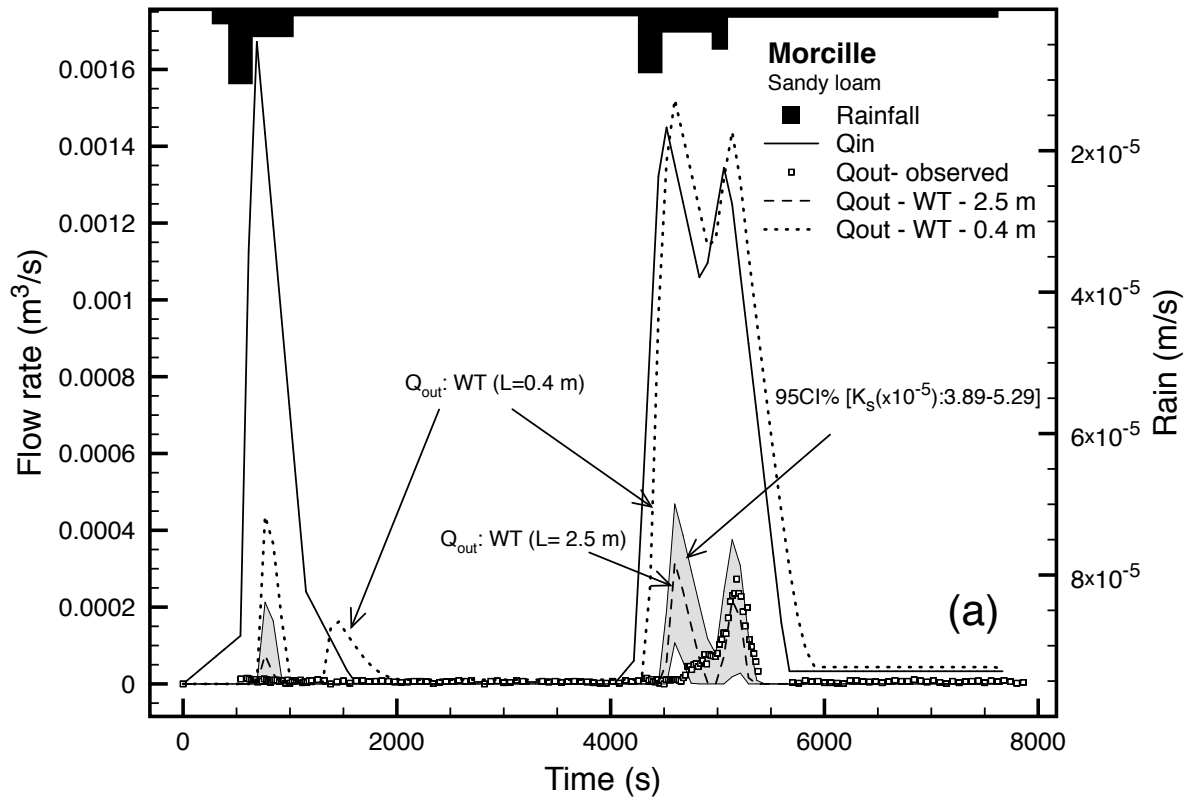
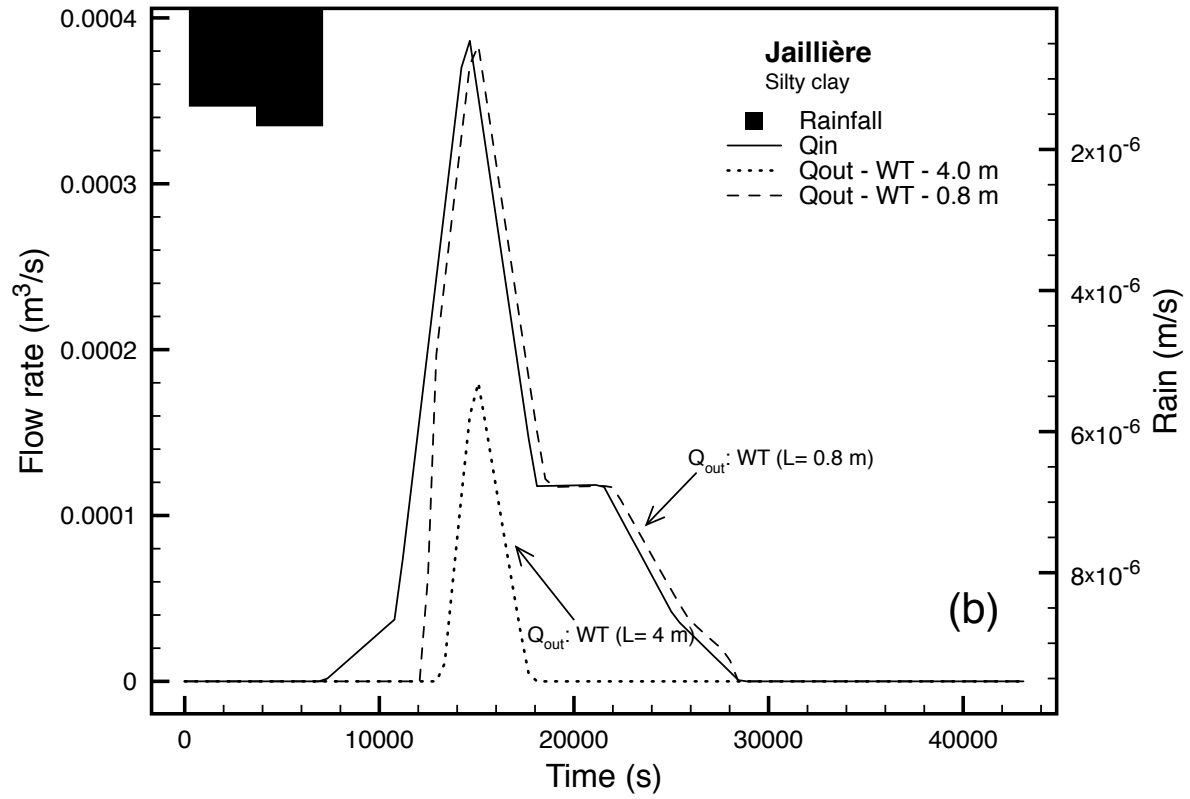


FIG. 4

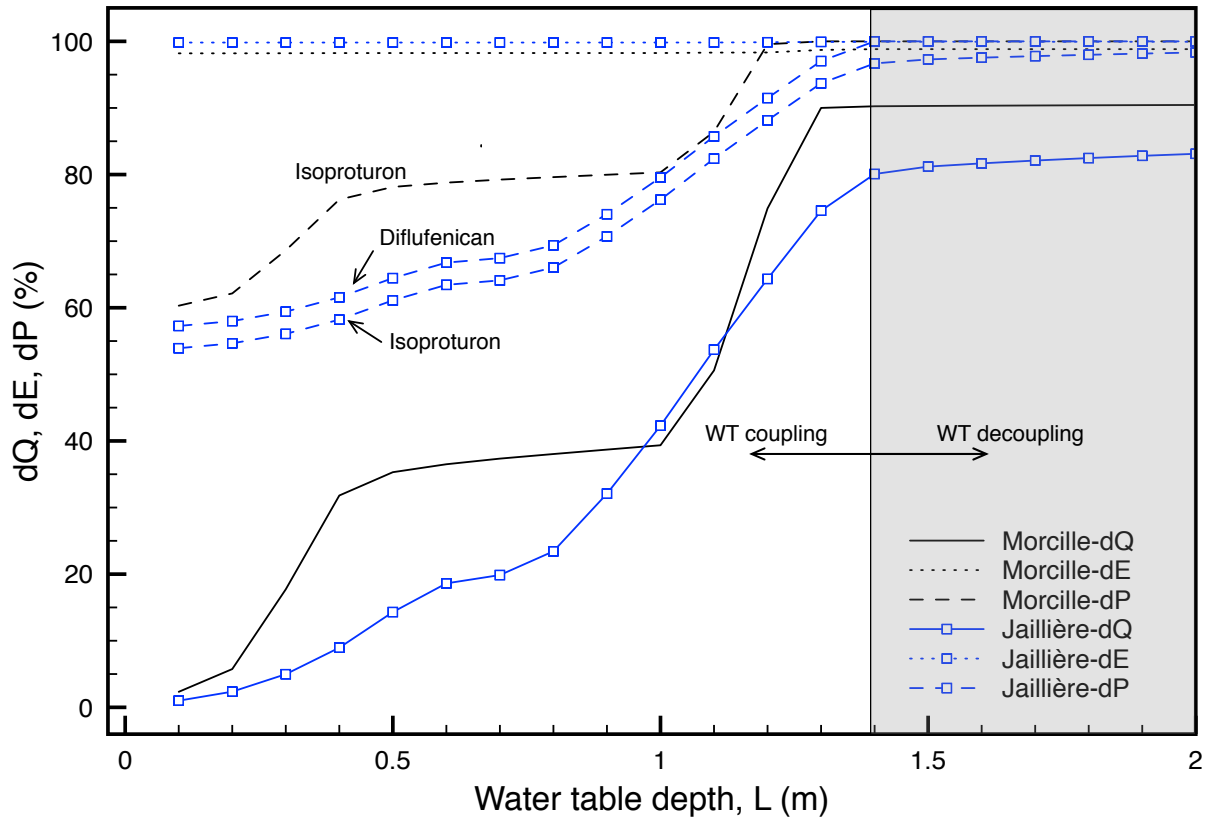


FIG. 5

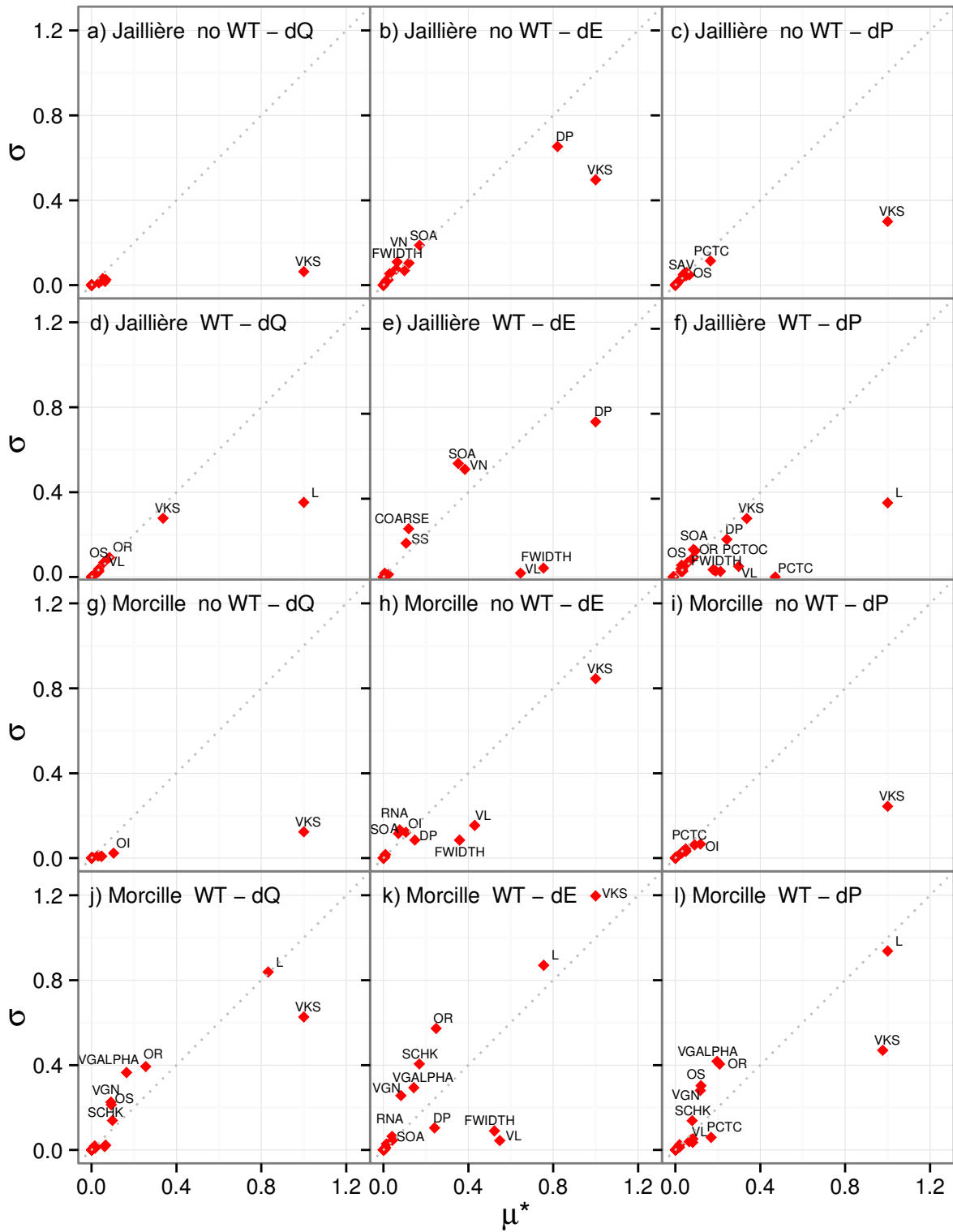


FIG. 6

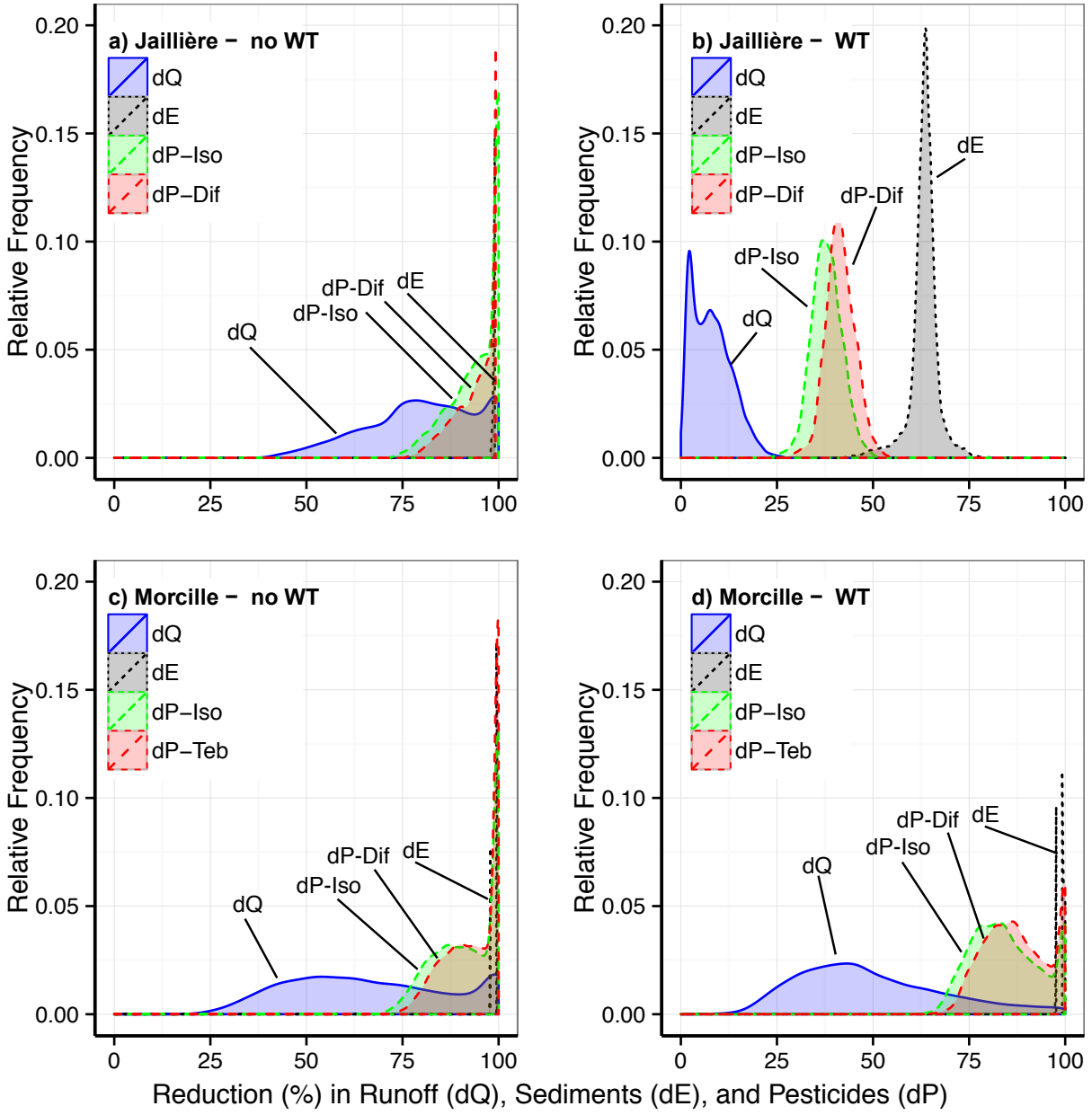


FIG. 7